J|A|C|S
ARTICLES
Published on Web 01/21/2004

Elucidation of the Electron Transfer Reduction Mechanism of Anthracene Endoperoxides

Robert L. Donkers† and Mark S. Workentin*

Contribution from the Department of Chemistry, The University of Western Ontario, London, ON, Canada, N6A 5B7

Received April 28, 2003; E-mail: mworkent@uwo.ca

Abstract: The homogeneous and heterogeneous reductions of the endoperoxides 9,10-diphenyl-9,10-epidioxyanthracene (**DPA-O_2**) and 9,10-dimethyl-9,10-epidioxyanthracene (**DMA-O_2**) were investigated, and they were found to undergo a dissociative electron-transfer reduction of the O−O bond to yield a distonic radical anion, with no evidence for C−O bond dissociation. A number of thermochemical parameters for each were determined using Savéant's model for dissociative electron transfer (ET), including E°, $\Delta G_o^\ddagger$, and bond dissociation energies. The products of the ET are dependent on the mode of reduction, namely heterogeneous or homogeneous, and on the electrode potential or standard potential of the homogeneous donor, respectively. The dissociative reduction of **DMA-O_2** under heterogeneous and homogeneous conditions yields the corresponding 9,10-dihydroxyanthracene **DMA-$(OH)_2$**, quantitatively, in an overall two-electron process. In the case of **DPA-O_2**, ET reduction also yields the corresponding 9,10-dihydroxyanthracene **DPA-$(OH)_2$** from reduction of the distonic radical anion, but in competition with this reduction, an *O*-neophyl-type rearrangement occurs that generates a carbon radical with a minimum rate constant of 5.9×10^{10} s^{-1}. In the presence of a sufficiently reducing medium, the carbon-centered radical is reduced ($E^\circ = -0.85$ V vs SCE) and ultimately yields 9-phenoxy-10-phenyl anthracene (**PPA**). The observation of this product is remarkable. In the heterogeneous ET, the yield of **DPA-$(OH)_2$/PPA** is 97:3 and allows an estimate of the rate constant for ET to the distonic radical anion. In homogeneous reductions, the *O*-neophyl rearrangement is quantitative, but the yield of **PPA** depends on the redox properties of the donor. A unified mechanism of reduction of **DPA-O_2** is presented to account for these observations.

Introduction

Anthracene endoperoxides exhibit interesting thermal and photochemical properties.[1−3] Their potential for reversible oxygen storage and as a chemical source of singlet oxygen, $^1O_2$ ($^1\Delta_g$), a species responsible for causing physiological damage, has made these compounds the subject of many fundamental investigations.[4−23] Typically, anthracenyl-type endoperoxides decompose thermally by two distinct reaction pathways. One pathway regenerates the parent aromatic hydrocarbon and oxygen in either the singlet or triplet state from a formal cycloreversion reaction, and the other generates products formed via homolytic cleavage of the O−O bond (Scheme 1).[6,12,23−40]

† Current address: Department of Physical Chemistry, University of Padova, via Loredan 2, 35131 Padova, Italy.

(1) Clennan, E. L.; Foote, C. S. In *Organic Peroxides*; Ando, W., Ed.; John Wiley & Sons: Chichester, England, 1992; pp 225−318.
(2) *Active Oxygen in Chemistry*; Foote, C. S., Valentine, J. S., Greenberg, A., Liebman, J. F., Eds.; Blackie Academic and Professional: New York, 1995; Vol. 2.
(3) *Active Oxygen in Biochemistry*; Foote, C. S., Valentine, J. S., Greenberg, A., Liebman, J. F., Eds.; Blackie Academic and Professional: New York, 1995; Vol. 3.
(4) Turro, N. J.; Chow, M. F. *J. Am. Chem. Soc.* **1981**, *103*, 7218−7224.
(5) Stevens, B.; Small, R. D., Jr. *J. Phys. Chem.* **1977**, *81*, 1605−1606.
(6) Sigman, M. E.; Zingg, S. P.; Pagni, R. M.; Burns, J. H. *Tetrahedron Lett.* **1991**, *32*, 5737−5740.
(7) Sitzmann, E. V.; Langan, J. G.; Hrovat, D. A.; Eisenthal, K. B. *Chem. Phys. Lett.* **1989**, *162*, 157−162.
(8) Schmidt, R.; Drews, W.; Brauer, H.-D. *J. Photochem.* **1982**, *18*, 365−378.
(9) Schmidt, R.; Drews, W.; Brauer, H.-D. *Z. Naturforsch. A* **1982**, *37*, 55−57.
(10) Schmidt, R.; Schaffner, K.; Trost, W.; Brauer, H.-D. *J. Phys. Chem.* **1984**, *88*, 956−958.
(11) Rigaudy, J.; Defoin, A.; Baranne-Lafont, J. *Angew. Chem., Int. Ed. Engl.* **1979**, *18*, 413−415.
(12) Rigaudy, J.; Breliere, C.; Scribe, P. *Tetrahedron Lett.* **1978**, *7*, 687−690.
(13) Kearns, D. R.; Khan, A. U. *Photochem. Photobiol.* **1969**, *10*, 193-210.
(14) Jesse, K. J. *Chem. Phys. Lett.* **1997**, *264*, 193−198.
(15) Jesse, J.; Comes, F. J. *J. Phys. Chem.* **1991**, *95*, 1311−1315.
(16) Jesse, J.; Markert, R.; Comes, F. J.; Schmidt, R.; Brauer, H.-D. *Chem. Phys. Lett.* **1990**, *166*, 95−100.
(17) Jesse, J.; Comes, F. J.; Schmidt, R.; Brauer, H.-D. *Chem. Phys. Lett.* **1989**, *160*, 8−12.
(18) Gudipati, M. S.; Klein, A. *J. Phys. Chem. A* **2000**, *104*, 166−167.
(19) Blumenstock, T.; Comes, F. J.; Schmidt, R.; Brauer, H.-D. *Chem. Phys. Lett.* **1986**, *127*, 452−455.
(20) Brauer, H.-D.; Schmidt, R. *J. Phys. Chem. A* **2000**, *104*, 164−165.
(21) Eisenthal, K. B.; Turro, N. J.; Dupuy, C. G.; Hrovat, D. A.; Jenny, T. A.; Sitzmann, E. V. *J. Phys. Chem.* **1986**, *90*, 5168−5173.
(22) Ernsting, N. P.; Schmidt, R.; Brauer, H.-D. *J. Phys. Chem.* **1990**, *94*, 5252−5255.
(23) Aubry, J.-M.; Pierlot, C.; Rigaudy, J.; Schmidt, R. *Acc. Chem. Res.* **2003**, *36*, 668−675.
(24) Dufraisse, C.; Rocher, H. *Bull. Soc. Chim. Fr.* **1935**, 2235−2240.
(25) Dufraisse, C. *Bull. Soc. Chim. Fr.* **1936**, 1847−1872.
(26) Dufraisse, C.; Horclois, R. *Bull. Soc. Chim. Fr.* **1936**, 1894−1905.
(27) Dufraisse, C.; Le Bras, J. *Bull. Soc. Chim. Fr.* **1937**, *5*, 1037−1046.
(28) Dufraisse, C.; Velluz, L.; Velluz, M. *Bull. Soc. Chim. Fr.* **1937**, 1260−1264.
(29) Dufraisse, C.; Priou, R. *Bull. Soc. Chim. Fr.* **1939**, 1649−1656.
(30) Dufraisse, C.; Velluz, L. *Bull. Soc. Chim. Fr.* **1942**, 171−187.
(31) Dufraisse, C.; Mathieu, J. *Bull. Soc. Chim. Fr.* **1947**, 307−310.
(32) Aksnes, G.; Vagstad, B. H. *Acta Chem. Scand.* **1979**, *B33*, 47−51.
(33) Bachmann, W. E.; Chemerda, J. M. *J. Chem. Soc.* **1939**, 116−118.
(34) Etienne, A. *Bull. Soc. Chim. Fr.* **1937**, 634−638.
(35) Etienne, A.; Staehelin, A. *Bull. Soc. Chim. Fr.* **1954**, 748−754.
(36) Etienne, A.; Lepeley, J.-C.; Heymès, R. *Bull. Soc. Chim. Fr.* **1949**, 835−840.

10.1021/ja035828a CCC: $27.50

Scheme 1. Competitive Reaction Pathways in the Thermal and Photochemical Activation of 9,10−Epidioxyanthracences

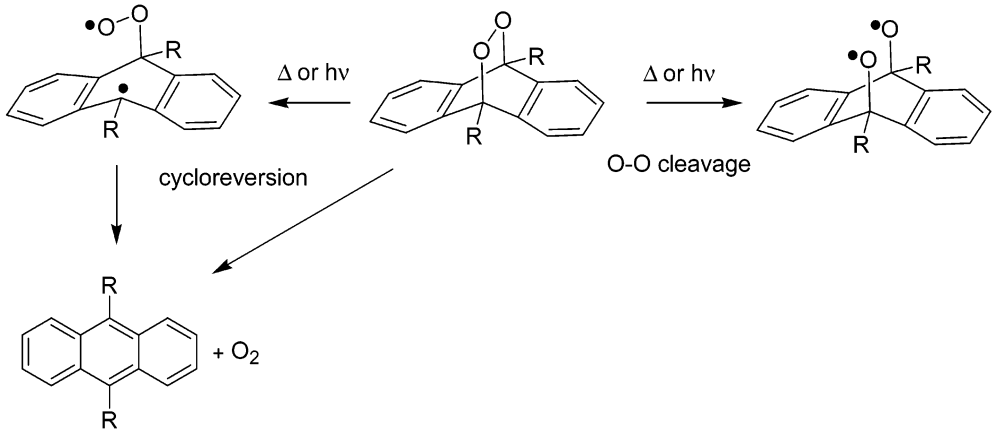

The relative yields of these two reaction processes have been studied as a function of structure and experimental conditions to ascertain the mechanism and activation parameters for a number of systems.

The thermolysis of a prototypical aromatic endoperoxide, namely 9,10-diphenyl-9,10-epidioxyanthracene (**DPA-O_2**), in chlorobenzene yields only products from the cycloreversion, whereas when the substituents at the bridgehead are not phenyl the amount of products from cleavage of the O−O bond and subsequent rearrangement increases. Rigaudy and co-workers were first to report[12] the photolysis of **DPA-O_2**. **DPA-O_2** has two UV−vis absorption bands, a high energy absorption centered at 254 nm, and less intense low-energy absorption at wavelengths above 350 nm. They discovered that irradiation with 254-nm light leads to cycloreversion while irradiation at the low-energy absorption leads to products arising from O−O homolytic cleavage, including the diepoxide and products derived from it. The homolytic cleavage to yield the biradical is reversible, and thus reformation of the endoperoxide competes with other reactions of the biradical. Kearns and Khan[13] predicted this dual reactivity using orbital correlation diagrams for the 1,4-cyclohexadiene endoperoxide and generalized that these observations should apply to the endoperoxides of all aromatic hydrocarbons. The photochemical behavior for the endoperoxides of aromatic molecules was investigated by Brauer and co-workers, who observed the dual reactivity as a general occurrence in these systems.[8−10,20,22,41] Investigation of the photocycloreversion reaction by Brauer and co-workers using femtosecond laser flash photolysis techniques supports the hypothesis of a two-step process. The first step in their proposed mechanism involves the barrierless C−O cleavage to form a biradical in competition with internal conversion. Next, the second C−O cleavage occurs to extrude $^1O_2$ in the rate-determining step.[7,14−17,19,22] Recent computational and experimental investigations of this mechanism by Klein and co-workers dispute Brauer assignments of the excited states involved in the competing processes.[42] This was followed with some discussion from both sides of this issue in the literature.[18,20] Currently, the assignment of the excited states is open to debate, and an excellent account of the reversible binding of oxygen to aromatic compounds has recently appeared.[23]

Photochemical reaction mechanisms and dissociative electron transfer (ET) mechanisms are often similar in their fate. For example, photolysis of sigma bonds of molecule A−B can result in homolysis into A$^\bullet$ and B$^\bullet$. ET reduction of A−B often results in an analogous fragmentation into A$^\bullet$ and B$^-$, the only difference being the extra charge on the B fragment. Examples of these include the reduction of C−X where X is a halogen,[43−46] or O−O bonds[2,3,47−52,54−56] of peroxides and endoperoxides. In the case of alkyl endoperoxides such as ascaridole, both photolysis and ET lead to O−O bond fragmentation.[51−53] In the alkyl endoperoxide cases we studied using direct electrochemical methods, ET leads to a concerted dissociative fragmentation of the O−O bond to yield a distonic radical anion $^\bullet$O−R−R−O$^-$ (eq 1) that is reduced in a second ET (eq 2) to ultimately yield the *cis*-diol; i.e., no reactivity resulting from the alkoxy radical fragment is observed.

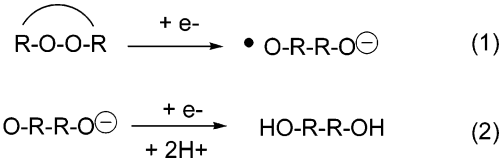

Because of our interest in the ET reactions of peroxides and endoperoxides,[47,49−52,54−56] we investigated the ET chemistry of two model aromatic endoperoxides, namely, 9,10-diphenyl-

(37) Willemart, A. *Bull. Soc. Chim. Fr.* **1937**, 510−517.
(38) Willemart, A. *Bull. Soc. Chim. Fr.* **1937**, 357−363.
(39) Willemart, A. *Bull. Soc. Chim. Fr.* **1938**, 557−563.
(40) Southern, P. F.; Waters, W. A. *J. Chem. Soc.* **1960**, 4340−4346.
(41) Drews, W.; Schmidt, R.; Brauer, H.-D. *Chem. Phys. Lett.* **1980**, *70*, 84.
(42) Klein, A.; Kalb, M.; Gudipati, M. S. *J. Phys. Chem. A* **1999**, *103*, 3843−3853.
(43) Savéant, J.-M. In *Advances in Physical Organic Chemistry*; Tidwell, T. T., Ed.; Academic Press: London, 2000; Vol. 35, pp 117−192.
(44) Savéant, J.-M. In *Advances in Electron-Transfer Chemistry*; Mariano, P. S., Ed.; JAI Press: Greenwich, CT, 1994; pp 53−115.
(45) Savéant, J.-M. *J. Am. Chem. Soc.* **1992**, *114*, 10595−10602.
(46) Savéant, J.-M. *J. Am. Chem. Soc.* **1987**, *109*, 6788−6795.
(47) Workentin, M. S.; Maran, F.; Wayner, D. D. M. *J. Am. Chem. Soc.* **1995**, *117*, 2120−2121.
(48) Antonello, S.; Musumeci, M.; Wayner, D. D. M.; Maran, F. *J. Am. Chem. Soc.* **1997**, *119*, 9541−9549.
(49) Donkers, R. L.; Maran, F.; Wayner, D. D. M.; Workentin, M. S. *J. Am. Chem. Soc.* **1999**, *121*, 7239−7248.
(50) Magri, D. C.; Workentin, M. S. *Org. Biomol. Chem.* **2003**, *1*, 3418−3429.
(51) Workentin, M. S.; Donkers, R. L. *J. Am. Chem. Soc.* **1998**, *120*, 2664−2665.
(52) Donkers, R. L.; Workentin, M. S. *Chem.−Eur. J.* **2001**, *7*, 4012−4020.
(53) Maheshwari, K. K.; de Mayo, P.; Wiegand, D. *Can. J. Chem.* **1970**, *48*, 3265−3268.
(54) Donkers, R. L.; Workentin, M. S. *J. Phys. Chem.* **1998**, *102*, 4061−4063.
(55) Magri, D. C.; Donkers, R. L.; Workentin, M. S. *J. Photochem. Photobiol., A* **2001**, *138*, 29−34.
(56) Donkers, R. L.; Tse, J.; Workentin, M. S. *J. Chem. Soc., Chem. Commun.* **1999**, 135−136.

9,10-epidioxyanthracene, **DPA-O$_2$** and 9,10-dimethyl-9,10-epidioxyanthracene, **DMA-O$_2$**. Our other studies indicated that upon ET, it is the O−O bond that is the dissociating bond. However, part of the initial interest in the ET chemistry of **DPA-O$_2$** was to investigate whether the dual reactivity observed in the thermal and, in particular, photochemical studies of aromatic endoperoxides extended to ET-initiated reactions. A pertinent example addressing this question for aromatic endoperoxides was reported by Amatore and Brown.[57] In an elegant study emphasizing paired electrosynthesis on a femtoliter scale, they proposed that the endoperoxide 9,10-dihydro-9,10-epidioxyanthracene is the initial product formed in the reaction between the anthracene radical cation and superoxide anion. They proposed that the product ultimately isolated, 9,10-anthracenedione, is formed by ET-initiated O−O fragmentation of 9,10-dihydro-9,10-epidioxyanthracene, although they did not provide any mechanistic details of the ET process itself.

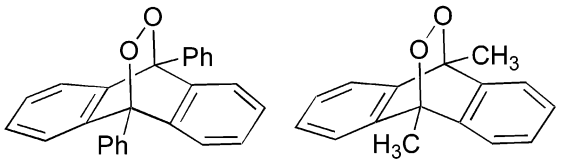

DPA-O$_2$ **DMA-O$_2$**

In a previous communication,[56] we reported that ET to **DPA-O$_2$** results in a dissociative ET fragmentation of the O−O bond to yield a distonic radical anion ($^{\bullet}$O−R−R−O$^-$), similar to our observations with other endoperoxides.[51,52,54] However, in the cyclic voltammogram (CV) of the reduction of **DPA-O$_2$**, the redox process of 9-phenoxy-10-phenyl anthracene (**PPA**) was observed. We proposed that this product arose from an unprecedented *O*-neophyl-type rearrangement of the distonic radical anion, $^{\bullet}$O−R−R−O$^-$, in competition with its reduction to yield the corresponding 9,10-diol, **DPA-(OH)$_2$**. The relative yield of the products from these competing pathways, determined from preparative scale electrolyses, depended on the potential of the reduction. However, specific details of the mechanism were not elucidated. In this paper, we now present the results of an extensive study of the heterogeneous and homogeneous ET reduction of **DPA-O$_2$** and **DMA-O$_2$**. The results allow for a unified description of the mechanism of reduction of **DMA-O$_2$** and, more specifically, **DPA-O$_2$**. In addition to providing an important new example of dissociative ET to a biologically important class of compounds, the analysis of the mechanism suggests that systems such as these can be developed as kinetic probes, or "clocks", for ET reactions of distonic radical anions.

Results

Cyclic Voltammetry of DPA-O$_2$ and DMA-O$_2$. Electrochemical reduction of **DMA-O$_2$** and **DPA-O$_2$** is investigated using cyclic voltammetry at a glassy carbon working electrode in acetonitrile (ACN) and *N*,*N*-dimethylformamide (DMF) solutions containing 0.1 mol·L^{-1} tetraethylammonium perchlorate; representative voltammograms are shown in Figures 1 and 2, respectively. For **DMA-O$_2$**, the peak potentials (E_p) at 0.1 V·s^{-1} are −1.27 and −1.34 V vs SCE in ACN and DMF,

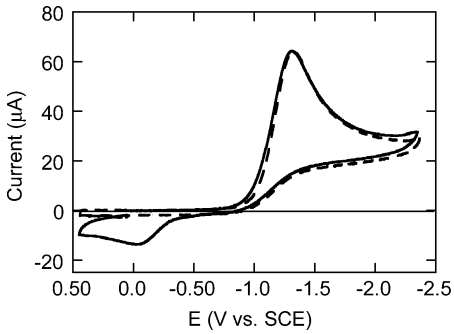

Figure 1. Cyclic voltammogram at 0.2 V·s^{-1} of 2 mmol·L^{-1} **DMA-O$_2$** in DMF with 0.1 mol·L^{-1} TEAP. Dashed line is in the presence of 4 mmol·L^{-1} 2,2,2-trifluoroethanol.

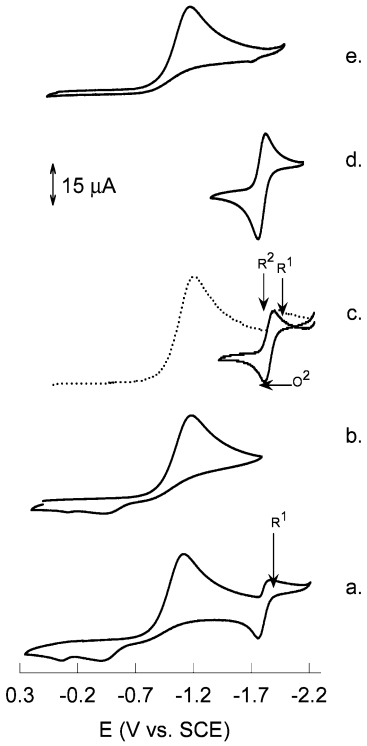

Figure 2. (a) Cyclic voltammogram of 2.03 mmol·L^{-1} **DPA-O$_2$** in DMF with 0.1 mol·L^{-1} TEAP. (b) Voltammograms switching before reversible product wave. (c) Voltammogram that cycles through the reversible couple of the PPA product. (d) Voltammogram that cycles through the reversible couple of the PPA product after holding the electrode potential at the negative vertex −2.1 V vs SCE for 30 s. (e) Voltammogram in the presence of 10 equiv of 2,2,2-trifluoroethanol. ALL CVs were measured at 0.2 V·s^{-1}.

respectively, and for **DPA-O$_2$** the potentials are −1.06 and −1.21 V vs SCE. As the scan rate is increased, the E_p values shift to more negative values and the peaks become broader. The peak heights that are normalized for scan rate also decrease as the scan rate is increased. The transfer coefficient (symmetry factor), α, is a measure of how the activation free energy, $\Delta G^{\ddagger}$, varies as a function of the driving force for ET, ΔG^{ET},[58] namely, $\alpha = \partial\Delta G^{\ddagger}/\partial\Delta G^{ET}$. Average values of α are calculated from the shift of the peak potential with scan rate, and they are 0.25 and

(57) Amatore, C.; Brown, A. R. *J. Am. Chem. Soc.* **1996**, *118*, 1482−1486.

(58) More correctly, the α, $E°$, and k_{het} values obtained are "apparent values" because they are not corrected for the ohmic drop due to charging of the electric double layer. For example α is related to its apparent value by $\alpha = \alpha_{app}\{1 - (d\phi^{\ddagger}/dE)\}$. Since the double layer properties of glassy carbon are not well-known, the correction cannot be made. However, it has been suggested that the correction is small or negligible. Regardless, the apparent data obtained has been shown to provide a reasonable estimate of the actual parameters.

Table 1. Voltammetric Data for the Reduction of **DPA-O$_2$** and **DMA-O$_2$** in DMF and ACN at 25 °C with 0.1 mol·L^{-1} TEAP Electrolyte Measured by Cyclic Voltammetry at a Glassy Carbon Working Electrode

	ν	DPA-O$_2$		DMA-O$_2$	
	(V·s^{-1})	ACN	DMF	ACN	DMF
E_p (V vs SCE)	0.1	−1.06	−1.21	−1.27	−1.34
	1.0	−1.17	−1.37	−1.37	−1.44
	5.0	−1.21	−1.41	−1.49	−1.53
	10	−1.25	−1.47	−1.50	−1.61
E_p vs log ν slope (mV·decade^{-1})		96	122	107	117
$\alpha_{app} = (RT/nF)(d\ln \nu/dE_p)$		0.32	0.25	0.26	0.27
$\alpha = 1.85(RT/F)(E_{p/2} - E_p)$	0.1	0.34	0.26	0.32	0.31
	1.0	0.28	0.24	0.29	0.29
	5.0	0.25	0.20	0.27	0.28
	10	0.23	0.19	0.25	0.26
n (F·mol^{-1}) no acid		1.94	2.00	1.93	1.99
n (F·mol^{-1}) acid		1.89	2.11	2.07	2.01

0.27 for **DPA-O$_2$** and **DMA-O$_2$** in DMF, respectively; similar values are found in ACN. The corresponding values calculated from the peak widths decrease with increasing scan rate and are consistent with the values calculated from the peak potential shift. Values of α in this range indicate that the initial ET controls the electrode kinetics and are used as a diagnostic criterion to suggest a concerted dissociative ET, where the ET and bond cleavage occur simultaneously.[43,44] A summary of the peak potentials, peak widths as a function of scan rate, and α values along with the equations used to calculate them is provided in Table 1.

On the backward, positive potential scan, poorly defined irreversible oxidation waves are observed at −0.12 and −0.19 V vs SCE at 0.5 V·s^{-1} in ACN and DMF for **DMA-O$_2$**. Similar broad and undefined waves are observed for **DPA-O$_2$** in ACN at −0.34 and −0.24 V vs SCE. These oxidation peaks disappeared in the presence of nonnucleophilic acids such as 2,2,2-trifluoroethanol or acetanilide. Unfortunately, scanning through these peaks results in poisoning of the electrode surface, and the oxidation waves are unable to be quantified further.

The results of coulometric studies from preparative scale electrolyses carried out in the potential regions of the broad irreversible waves on a reticulated vitreous carbon working electrode are summarized in Table 1. At these potentials, electrolysis leads to the consumption of approximately 2 F·mol^{-1}, or two-electron equivalents, in either solvent in the presence and absence of non-nucleophilic weak acids, TFE, or acetanilide. For **DMA-O$_2$**, workup and isolation of the electrolysis mixture quantitatively yield the corresponding *cis*-diol, namely, *cis*-9,10-dimethyl-9,10-dihydro-9,10-dihydoxyanthracene, **DMA-(OH)$_2$**. In the electrolysis of **DPA-O$_2$**, a 97% yield of the *cis*-diol, *cis*-9,10-diphenyl-9,10-dihydroxyanthracene, **DPA-(OH)$_2$**, is isolated. The remaining 3% of the yield is **PPA.** The yield of these two products is independent of the applied potential between −1.1 and −1.5 V vs SCE. The molecular structure of **PPA** is verified using X-ray crystallography, and the relevant data is included in the Supporting Information.

The broad irreversible waves observed for the reduction of **DMA-O$_2$** and **DPA-O$_2$** are very similar to those previously observed for the reduction of the endoperoxides ascaridole, dihydroascaridole, and artemisinin studied by us[51,52,54,55] as well as acyclic peroxides studied by us[47,49,50] and others.[48,59] The combined preparative electrolysis and voltammetric analysis are consistent with a dissociative ET reduction of the O−O bond to form the distonic radical anion, followed by ET reduction to formally yield the dialkoxide dianion. The poorly defined oxidation waves are in the potential region expected for the oxidation of the alkoxide anions formed on the forward scan and correspond to the oxidation of these alkoxide anions.

Determination of the Heterogeneous ET Reduction Kinetics and Thermochemical Parameters. The heterogeneous ET rate constants (k_{het}) for the reduction of **DPA-O$_2$** and **DMA-O$_2$** are determined using the method of convolution potential sweep voltammetry. The theoretical and experimental treatment of this technique and its application to the determination of thermochemical parameters related to dissociative ET reductions has been described in detail elsewhere and are also provided in the Supporting Information.[48,60−63] Briefly, the experiment involves the careful acquisition of background-subtracted linear voltammetric scans of the dissociative ET waves in Figures 1 and 2b followed by evaluation of the waves according to the convolution integral that gives the convolution current (I), which is related to the real current (i) through the convolution integral, versus E curves. The $I-E$ plots have the limiting current corresponding to the diffusion-controlled conditions. From the sigmoid-shaped convolution data, the diffusion coefficients (D) in ACN and DMF with 0.1 mol·L^{-1} TEAP for **DPA-O$_2$** are calculated to be 1.2×10^{-5} and 4.0×10^{-6} cm^2·s^{-1} and those for **DMA-O$_2$** are 1.8×10^{-5} and 8.1×10^{-6} cm^2·s^{-1}, respectively.[64] The generally smaller D value for **DPA-O$_2$** compared to **DMA-O$_2$** is a reflection of a significant contribution to the molecular volume from the phenyl rings at the 9 and 10 positions. When the back electrode process is not observed (as in the present case), the k_{het} is related to i and I by the equation $\ln k_{het} = \ln D^{1/2} - \ln\{[I_{lim} - I(t)]/i(t)t\}$, and this k_{het} can be evaluated at each potential. Activation-driving force relationships are determined from the convolution data that relate k_{het} to the electrode potential. The curvature of the activation-driving force relationship is then used to quantitatively determine how the α changes as a function of the electrode potential, where $\alpha = -(RT/F)(d\ln k_{het}/dE)$.[48] Figures of the convolution data extracted from voltammetric data are provided in the Supporting Information. The α values determined from these data are consistently below 0.32 and decrease as potential moves toward negative potentials, consistent with the average α values reported in Table 1. Several thousand determinations of α are determined, and the linear trend of these values as a function of potential (or reaction energy) is evaluated and expressed as $\alpha = 0.73 + 0.40E$ for **DPA-O$_2$** and $\alpha = 0.67 + 0.29E$ for **DMA-O$_2$**. With these linear equations, the standard dissociative reduction potentials, $E^o_{ROOR/\cdot ORRO^-}$, for each is estimated by extrapolating to the potential value at $\alpha = 0.5$ that is the value defined for $\Delta G^{ET}_o = 0$ for most outer-sphere or dissociative ETs; the $E^o_{ROOR/\cdot ORRO^-}$ values are reported in Table 2. Values of the

(59) Kjær, N. T.; Lund, H. *Acta Chem. Scand.* **1995**, *49*, 848−852.
(60) Imbeaux, J. C.; Savéant, J.-M. *J. Electroanal. Chem.* **1973**, *44*, 169−187.
(61) Savéant, J.-M.; D, T. *J. Electroanal. Chem.* **1975**, *65*, 57.
(62) Antonello, S.; Maran, F. *J. Am. Chem. Soc.* **1998**, *119*, 12595−12600.
(63) Maran, F.; Workentin, M. S.; Wayner, D. D. M. In *Advances in Physical Organic Chemistry*; Tidwell, T. T., Richard, J. P., Eds.; Academic Press: San Diego, CA, 2001; Vol. 36, pp 85−166.
(64) The change from ACN to DMF is expected to decrease the D value by a value equal to the square root of the ratio of the two viscosities, which is 1.53. The ratio of D obtained with **DMA-O$_2$** is 1.49 and **DPA-O$_2$** is 1.73. The latter value is a bit high, and we believe it is the result of the D value in DMF being underestimated because of some interaction between the radical with the solvent.

Table 2. Summary of the Thermochemical Parameters for **DPA-O$_2$** and **DMA-O$_2$** along with Three Model Compounds: Ascaridole, Di-*tert*-butylperoxide, and Bis(triphenylmethyl)peroxide

	DPA-O$_2$	**DMA-O$_2$**	ascaridole[a]	$(CH_3)_3CO–OC(CH_3)_3$[b,c]	$Ph_3CO–OCPh_3$[c]
$E^o_{ROOR/\cdot ORRO^-}$ (V vs SCE)	−0.56	−0.56	−1.3	−1.48 (DMF) −1.55 (ACN)	−1.13
log k^o_{het} (cm s^{-1})	−4.9	−4.4	−5.9	−6.1	
r_{eff}[d] (Å)	3.68	3.92	2.76	2.72	3.83
$\Delta G^{\ddagger}_o$ (kcal·mol^{-1})	7.19	9.83	11.9	13.08	
$\lambda^{(Marcus)}$[f] (kcal·mol^{-1})	10.4	13.1	13.9	14.1	10.0
BDE (estimated) (kcal·mol^{-1})	16.3[e]	23.2[e]	28.5	37.3	31.4

[a] Reference 52. [b] References 47 and 49. [c] Reference 48. [d] Reference 61. [e] Determined by using the Marcus λ and the intrinsic barrier predicted using the Savéant model. We believe these to be lower limits. [f] $\lambda = \{(e^2/4\pi\epsilon^o)(1/\epsilon_{op} - 1/\epsilon_s)(1/nr_{eff})\}$ where e is the charge of the electron, ϵ_{op} and $/\epsilon_s$ are the high frequency and static dielectric constant of the solvent, r_{eff} is the effective radius, and $n = 4$.

standard heterogeneous rate constant, k^o_{het}, are obtained by extrapolation of the activation-driving force relationship to the newly determined $E^o_{ROOR/\cdot ORRO^-}$ value. Values for k^o_{het} for concerted dissociative ET reactions are determined to be 1.3×10^{-5} and 4.0×10^{-5} cm·s^{-1} for **DPA-O$_2$** and **DMA-O$_2$**, respectively. These small values support the rate-determining nature of the initial ET. The consistency of the k^o_{het} and $E°$ values are checked by digital simulation of the cyclic voltammograms, which adequately reproduce the experimental curves.

Application of Savéant's model of concerted dissociative ET (eq 3) to the trend of the α data with electrode potential provides the intrinsic free-energy barrier of the reaction, $\Delta G^{\ddagger}_o$. This model can be further broken down into contributions from the bond dissociation energy (BDE) and solvating energy, λ, such that $\Delta G^{\ddagger}_o = (\lambda + BDE)/4$. From the slopes of the equations for α above, the $\Delta G^{\ddagger}_o$ values for **DPA-O$_2$** and **DMA-O$_2$** are evaluated to be 7.14 and 9.83 kcal·mol^{-1}, respectively. Because of the nature of the experiments and the inherent errors (100−200 mV), we believe these are lower limits. There are no reliable estimates for either the BDE or solvating energies, λ, for either of these systems available in the literature. It is possible to estimate the λ using the solvent cavity models of Marcus.[44] A summary of the equation used and the value determined is shown in Table 2. The Marcus estimation is used selectively over other models of Hush and Kojima−Bard because the latter two are shown in other dissociative systems to significantly overestimate λ and thus lead to underestimates of the BDE value. **DPA-O$_2$**, for example, has BDE values of 7.96 and 13.3 kcal·mol^{-1}, respectively, using the Hush and Kojima−Bard values. Using the λ values of Marcus's method, along with $\Delta G^{\ddagger}_o$, we calculate estimates of 16.3 and 23.2 kcal·mol^{-1} for the BDE of **DPA-O$_2$** and **DMA-O$_2$**, respectively. Analysis of the intrinsic barrier for these endoperoxides is consistent with the differences in the BDE values and the larger calculated solvating energies for **DMA-O$_2$**. The effective solvating radius (r_{eff})[65] for **DMA-O$_2$** is much smaller than **DPA-O$_2$**, and this is reflected in higher values of the solvating energy. The larger r_{eff} for **DPA-O$_2$** is a result of the two outer phenyl rings that can provide extra shielding to any charge formed.

$$\Delta G^{\ddagger} = \frac{\lambda + BDE}{4}\left(1 + \frac{\Delta G^{ET}}{(\lambda + BDE)}\right)^2 \qquad (3)$$

Cyclic Voltammetry of DPA-O$_2$. The most intriguing aspect of the cyclic voltammetry of **DPA-O$_2$** that is not seen with other endoperoxides or peroxides we have studied to date is the observation of a reducible product at a more negative potential than the dissociative reduction wave (Figure 2a). In this expanded potential region, there is a second reduction that is much smaller in current than the initial broad reduction wave. This second reduction wave, which we label as R^1, becomes increasingly more broad and less defined and shifts to negative potential as the scan rate is increased until it completely disappears at a scan rate of 75 V·s^{-1}. On the return scan a well-defined oxidation peak is observed; this we label as O^2. In Figure 2c, the forward scan, shown with the dashed line, is the same as the forward scan in Figure 2a. The return scan, represented with the solid line in Figure 2c, passes through peak O^2 and then switches potential direction again. On the second scan in the negative direction, a new reduction peak is observed, R^2, that is clear and well-defined. Qualitatively, it appears that R^1 is related to the reversible couple, R^2 and O^2. At the lowest scan rates investigated, the peak potential of R^1 is the same as the peak potential of R^2; however, the shape of the peaks and their behavior with increased scan rate are different. Figure 2d shows a cyclic voltammogram that starts at the potential of ~ -2.1 V and then scans through O^2 and R^2. Under this condition, R^2 and O^2 are well-defined at all scan rates, and from analysis of peak data they represent a redox couple of a single compound with standard potentials of −1.76 and −1.80 V vs SCE in ACN and DMF, respectively. When preparative electrolysis is carried out at the potential equivalent to R^1 or R^2, a *quantitative* yield of **PPA** is isolated; the redox couple R^2/O^2 corresponds to the reduction and oxidation of **PPA**. The amount of the **PPA** formed in the cyclic voltammetry experiment (estimated from the peak current) in Figure 2d depends on the scan rate and the time the potential is held at values more negative than ca. −1.9 V vs SCE; the amount of product reaches a maximum value for times greater than 25 s.

The amount of **PPA** observed in the voltammogram, indicated by the current measurement of the R^2/O^2 couple in the cyclic voltammetry, is investigated in the presence of several different

(65) The solvating energy, λ_{het}, was estimated using solvent cavity model by Marcus and the effective radii approach for concerted dissociative ET systems. In these expressions, the heterogeneous reorganization energy depends only on the structure of the endoperoxide. It is crucial that the radius entered into these equations accurately represents the amount of volume that will require solvating upon electron transfer. The radii of **DPA-O$_2$** and **DMA-O$_2$** were determined using the density of the compound and the diffusion coefficients determined from the convolution experiment using the Stokes−Einstein equation. These radii were then transformed into their effective radii using the equation: $r = [r_B(2r_{AB} - r_B)/r_{AB}]$ where r_{AB} is the radius of the starting molecule and r_B is an estimate of the radius of the fragment receiving the charge. The developing charge in the ET upon O−O bond cleavage is expected to develop in only part of product, and the uncharged portion aids in screening the charge. In the case of these endoperoxides, the uncharged fragment is quite large and therefore the effective radii are expected to be significantly smaller than the uncorrected radii. The size of the reduced fragment is approximated by the triphenylmethyl alkoxide anion for **DPA-O$_2$** and the 1,1-diphenylethyl alkoxide anion for **DMA-O$_2$**. Both are similar to the anion that is generated in the ET.

Table 3. Summary of the Homogeneous ET Reduction of **DPA-O_2**, the Yield of **PPA** product in ACN and DMF, and the amount of charge consumed in the reduction

donor	$E°$ (V)[c] ACN	$E°$ (V)[c] DMF	**PPA** yield (%) ACN	**PPA** yield (%) DMF	n (F·mol^{-1})
9-phenoxy-10-phenylanthracene[a]	−1.78	−1.85	100	100	
2-nitrobiphenyl	−1.16	−1.19	95	91	1.99
nitrobenzene	−1.10	−1.10	97	94	2.07
2-nitroacetophenone	−0.96	−0.97	92	92	
2,3-dimethylanthraquinone	−0.93	−0.90	97	56	
anthraquinone	−0.87	−0.84	97	38	0.95
4-nitrobenzonitrile	−0.81	−0.79	0	3	1.02[d]
benz-a-anthracene-7,12-dione	−0.77	−0.71	29	9	1.07
tetrakis-4-nitrophenylethene[b]	−0.72	−0.69	39	15	
11,11′,12,12′-tetracyano-anthraquinodimethane[b]	−0.31	−0.26	0	0	

[a] Based on the peak height from cyclic voltammetry experiments compared to that of an authentic sample. [b] Two-electron donor. [c] V vs SCE. [d] Difficult to reproduce and quantify due to some loss of mediator during the experiment.

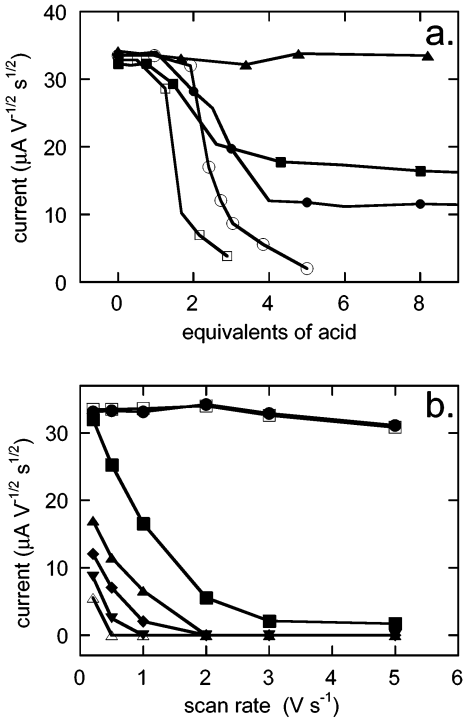

Figure 3. (a) Variation of the R^2 peak height normalized for scan rate in a cyclic voltammogram of **DPA-O_2** as a function of acid concentration. (▲) Acetanilide, (■) 2,6-di-*tert*-butyl phenol, (●) 1,1,1,3,3,3-hexafluoro-2-propanol, (○) 2,2,2-trifluoroethanol, and (□) phenol. Water and methanol were also used as acids and are coincident with the acetanilide data but were left off the plot. (b) Variation of the cyclic voltammetry R^2 peak height (normalized for scan rate) as a function of scan rate in the presence of (□) 0, (●) 1, (■) 2, (▲) 3, (◆) 5, (▼) 6, and (△) 8 equiv of 2,2,2-trifluoroethanol.

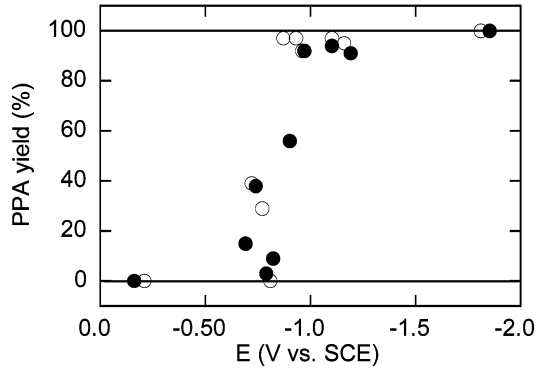

Figure 4. Yield of **PPA** from the homogeneous reduction of **DPA-O_2** as a function of donor oxidation potential in (○) ACN and (●) DMF.

organic acids. Acids with wide-ranging pK_a values and structural characteristics are chosen to determine a structure−reactivity relationship for the protonation reactions. The acids studied are 2,2,2-trifluoroethanol (TFE), 1,1,1,3,3,3-hexafluoro-2-propanol (HFIP), acetanilide, methanol, water, phenol, and 2,6-di-*tert*-butylphenol (DBP). The results indicate that the yield of **PPA** depends on the structure, pK_a, and concentration of the acid. Figure 2e shows a voltammogram of **DPA-O_2** acquired in the presence of 10 equiv of TFE. Under this condition, the initial broad dissociative wave is unchanged compared to that shown in Figure 2b, but the R^1, R^2, and O^2 product waves are essentially absent. Figure 3a shows the dependence of the peak current of R^2 measured at a scan rate of 0.2 V·s^{-1} as a function of relative concentration of these acids. There is no change in the peak current when acetanilide, water, or methanol is added at concentrations up to 10 equiv. The peak current drops sharply after the addition of 2 equiv of TFE and phenol, but less abruptly for HFIP and DBP, which did not completely eliminate the formation of **PPA** even after the addition of 10 equiv.

In Figure 3b, the peak current of R^2 is plotted as a function of scan rate for several different concentrations of TFE. For 1 and 2 equiv, there is no change in the peak current at any scan rate, indicating that at these concentrations there is no effect on the production of **PPA**. Once the concentration is increased above 2 equiv, the peak current drops sharply. This suggests that there is a competitive protonation process inhibiting the formation of **PPA**. After the addition of 5 equiv of TFE there is essentially no **PPA** at any scan rate, indicating trapping of an intermediate product.

Homogeneous Reduction of DPA-O_2. The yield of **PPA** in the heterogeneous reduction of **DPA-O_2** is found to be potential-dependent. For this reason, the reduction of **DPA-O_2** by a variety of homogeneous donors of varying oxidation potentials is studied in both ACN and DMF. This permitted the study of the ET to be extended to a broader free-energy range and allowed the nature of the donor to be changed. Aromatic radical anions ($D^{\bullet-}$) and dianions (D^{2-}) are used as outer sphere electron donors. The homogeneous donors chosen for study along with their standard potentials ($E°$) and the yield of **PPA** from the product studies are summarized in Table 3. The yield of **PPA** as a function of the oxidation potential of $D^{\bullet-}$ is also shown graphically in Figure 4. This figure illustrates that the formation of **PPA** also depends on the oxidation potential of the

Scheme 2. Mechanistic Pathways for the Electron Transfer Reduction of **DPA-O_2** and **DMA-O_2**

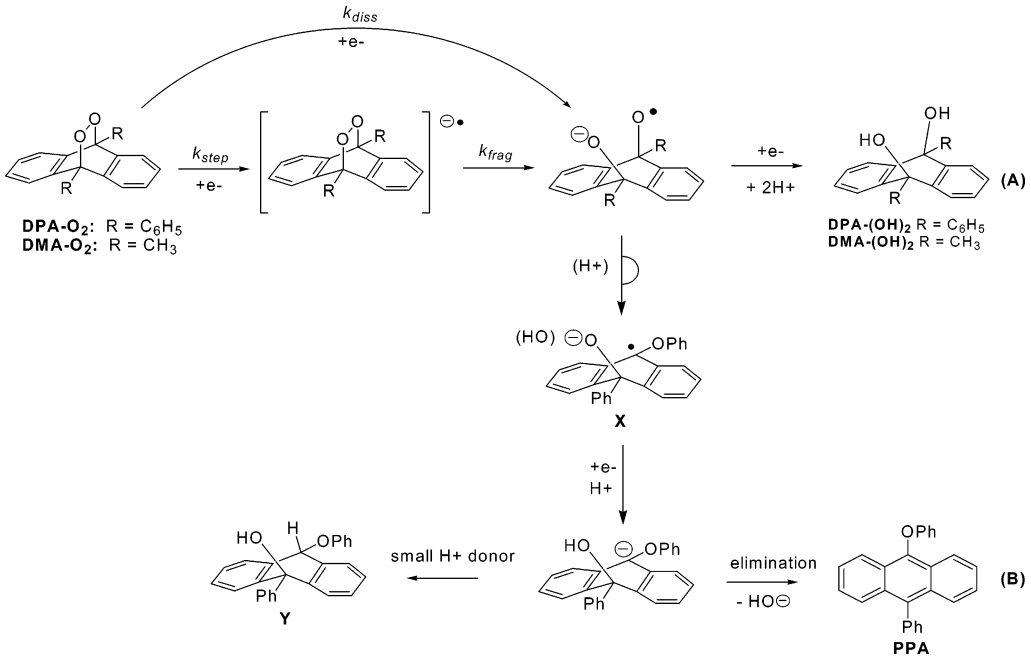

homogeneous donor. In none of the homogeneous reduction experiments is there evidence for the 9,10-diol, **DPA-$(OH)_2$**, the major product in the heterogeneous reduction. Under homogeneous reduction conditions at potentials more negative than −0.90 V vs SCE, the major product isolated is **PPA** in high yield. **PPA**, which is the minor product in the heterogeneous reduction, is also used as one of the homogeneous donors. When used as a homogeneous donor, the yield of **PPA** formed from **DPA-O_2** is quantitatively determined by the relative increase in the current measured for the **PPA** couple. This has ramifications on the mechanism of **DPA-O_2** reduction that will be discussed later.

At potentials less negative than −0.81 V vs SCE, the homogeneous reaction produces no **PPA**, but a number of other products including 9-hydroxyl-9-phenylanthrone, **HPA**, and other products derived from radical coupling. In this potential region, considerable mass is lost, and the recovered yields are always much lower than expected. Mixtures of products, including **PPA** in varying yields, are observed between the two potential regions, as summarized in Table 3 and illustrated in Figure 4. This allowed for the determination of the number of electrons involved in the reduction of **DPA-O_2**; for donors with oxidation potentials more negative than −0.95 V, the charge consumed is 2 F·mol^{-1} (two-electron equivalents), and for donors more positive than −0.81 V, the 1 F·mol^{-1} (one-electron equivalent) process occurs.

For comparison to the electrochemical homogeneous reductions, the reduction of **DPA-O_2** and **DMA-O_2** is also studied using ferrous chloride as a homogeneous chemical electron donor. These experiments result in a quantitative conversion of **DPA-O_2** to **HPA** and phenol, and **DMA-O_2** to 9-methyl-9-hydroxyanthrone (**HMA**). A catalytic amount of ferrous chloride is required for the conversion of **DPA-O_2**, whereas a stoichiometric amount is required to convert **DMA-O_2**.

Discussion

The discussion of the mechanism of reduction of **DPA-O_2** will focus on explaining cyclic voltammetry experiments shown in Figure 2. The broad irreversible two-electron wave corresponds to the dissociative reduction of the O−O bond, and its shape is governed by the slow ET kinetics. When heterogeneous electrolysis was carried out at a potential corresponding to the broad dissociative wave, 97% of the isolated material was the *cis*-diol, **DPA-$(OH)_2$**. This is consistent with a second heterogeneous ET to the alkoxyl radical portion of the distonic radical ion (or its protonated form) to form the dialkoxide dianion (or the 9-hydroxyl-10-alkoxide) product that is subsequently protonated upon workup according to path A in Scheme 2. The remaining 3% of the yield was **PPA**. This is in contrast to the heterogeneous reduction of **DMA-O_2** that quantitatively yields its corresponding *cis*-diol with no products formed that alter the 9,10-dimethyl anthracene carbon skeleton. The formation of **PPA** is consistent with an *O*-neophyl-type rearrangement of the alkoxyl radical portion of the distonic radical anion to form a carbon-centered radical (X) as depicted in path B of Scheme 2.

There are two limiting mechanisms possible for the dissociative ET reduction of the O−O bond. One is the concerted dissociative ET process, where electron uptake and bond breaking occur in a single step, as has been reported for a number of alkyl peroxides and endoperoxides. An alternative stepwise pathway involves ET to form a bound radical anion intermediate that fragments in a second step. As we have already stated, the voltammetric criteria are consistent with those generally accepted for a concerted dissociative ET.

If we assume a concerted reduction mechanism, then the formation of **PPA** arises from a competitive *O*-neophyl-type rearrangement of the alkoxyl radical portion of the distonic radical anion with its reduction. By way of comparison, the reduction potential of $Ph_3C-O^{\bullet}$ ($E^{\circ}_{Ph_3CO^{\bullet}/Ph_3CO^{-}}$) is −0.03 V vs SCE.[48] If we reasonably assume a similar reduction potential

for the distonic radical anion ($^{\bullet}O-R-R-O^{-}$, or its protonated form $^{\bullet}O-R-R-OH$), then it is being generated at the electrode at potentials more negative than −1.2 V, a favorable free energy of reaction of about −27 kcal/mol. If the rearrangement of the radical portion of the distonic radical anion intermediate is considered to be analogous to the *O*-neophyl-type rearrangement of the $Ph_3C-O^{\bullet}$ radical to the α-phenoxydiphenylmethyl radical investigated by Falvey et al., then the minimum rate constant can be assumed to be 5.9×10^{10} s^{-1}.[66] By using this value as an estimate of the rate of the rearrangement, then the observation of **PPA** in the heterogeneous reduction can serve as a clock for the rate constant of the second heterogeneous electron transfer (Scheme 2, path B). From the yield of **DPA-(OH)$_2$** and assuming that the $^{\bullet}O-R-R-O^{-}$ is formed within the electrode outer Helmholtz plane, which in DMF is ca. 5×10^{-8} cm, an estimate for k_{het} is on the order of 100 cm s^{-1}. This rate constant range is small for such a highly driven process. An unusually high reorganization energy associated with ET to $^{\bullet}O-R-R-O^{-}$ would slow the second ET, thus allowing the *O*-neophyl-type rearrangement to compete, although there is no apparent structural reason for this. Regardless, in the concerted ET mechanism we propose that the small amount of **PPA** produced resulted from a small amount of *O*-neophyl rearrangement along path B in Scheme 2.

Alternatively, in the stepwise mechanism, the voltammetric behavior can be described using an ECE mechanism (where E is an electrochemical step and C is a chemical step) with an initial ET step to form a bound radical anion intermediate that rapidly fragments in a second chemical step with a rate constant k_{frag} to form the distonic radical anion that can be reduced quickly to form the dialkoxide dianion (or $HO-R-R-O^{-}$). This stepwise mechanism can also account for the formation of **PPA** resulting from a competitive *O*-neophyl-type rearrangement of distonic radical anion to form the carbon-centered radical if k_{frag} is large enough that the majority of the distonic radical anion is generated ($^{\bullet}O-R-R-O^{-}$) at the electrode at the potential where the second ET is a highly driven process and be reduced very quickly. For the stepwise mechanism, the product distribution of **DPA-(OH)$_2$** and **PPA** would be an indication of the ratio of the rate constants for fragmentation to that of the *O*-neophyl-type rearrangement, $k_{frag}/k_{neophyl}$.[67] Using the rate constant of the *O*-neophyl rearrangement above and the measured 97:3 **DPA-(OH)$_2$**/**PPA** product ratio, we can estimate k_{frag} to be 1.8×10^{11} s^{-1}; a value almost on the order of a molecular vibration and thus at least being close to that being considered a concerted dissociative ET.

For **DMA-O$_2$**, the two-electron stoichiometry and quantitative conversion to the corresponding 9,10-diol are consistent with what is observed with the reduction of other endoperoxides and acyclic peroxides studied previously. Note that with this endoperoxide, the corresponding 1,2 methyl shift or β-scission reactions do not compete with the reduction of the distonic radical anion. Although the rate of the β-scission reaction is not known for $Ph_2MeCO^{\bullet}$, the rate constant of the 1,2 methyl shift rate is estimated to be 4.4×10^{6} s^{-1};[66] this provides a lower rate limit to compare the second heterogeneous ET.

The BDE values determined here are remarkably low, especially when the high thermal stability of these endoperoxides is considered. Because the BDE values are determined from the measured intrinsic barrier and an estimate of the λ (i.e., BDE $= 4\Delta G_o^{\ddagger} - \lambda$), the larger the estimated value of λ the lower the calculated BDE will be. Some stepwise character in the ET would also act to give low estimates of the BDEs using the approach here because in general, stepwise ET rate constants are larger and have a smaller intrinsic barrier than their concerted counterparts. Thus, we believe the BDE values reported here are lower limits and may be underestimated by a few kcal/mol. However, the general trend for acyclic peroxides is that phenyl substitution acts to lower the BDE and BDFE values.[48,63] For example, the values for bis(triphenylmethyl)peroxide are 7 kcal·mol^{-1} lower compared to its non phenyl substituted analogue, di-*tert*-butyl peroxide which has a BDE of 37 kcal·mol^{-1}.[47] The previously studied endoperoxides ascaridole and dihydroascaridole are reasonable nonphenyl analogues of the **DPA-O$_2$** and **DMA-O$_2$** endoperoxides and a similar drop in the bond energy values is noted in this series (Table 2). It should also be noted that the substituent effect on differences in the E° values between $(CH_3)_3COOC(CH_3)_3$ and $(Ph)_3COOC(Ph)_3$ is not unreasonable with the values of **DPA-O$_2$** and **DMA-O$_2$** compared to ascaridole.

For **DPA-O$_2$** under homogeneous reduction conditions, the isolated products are consistent with quantitative *O*-neophyl-type rearrangement; the difference here is that the $^{\bullet}O-R-R-O^{-}$ is not being generated at the electrode, and therefore, its reduction is limited by diffusion. **PPA** is formed quantitatively in a 2 F·mol^{-1} (two-electron equivalents) process when homogeneous donors with oxidation potentials more negative than −0.95 V are used. This is consistent with the carbon-centered radical, X, shown in Scheme 2, being reduced to its carbanion in this potential region. We should note that the intramolecular ET from the alkoxide anion to the carbon radical is an uphill process by about 19 kcal mol^{-1}. Donors with oxidation potentials positive of −0.81 V undergo a 1 F·mol^{-1} (one-electron equivalent) process presumably because the reduction of the carbon-centered radical does not occur at these potentials. Therefore, the center point of the transition region of the data in Figure 4 provides a reasonable estimate of the standard reduction potential of −0.85 V vs for the carbon-centered radical.[68] This value agrees well with estimates for other similar benzylic type radicals.[69,70] For example, the reduction potential of the diphenylmethyl (DPM) radical is −1.07 V vs SCE and that of the 9-phenoxyfluorenyl radical is −0.57 V vs SCE.[71] The slightly more positive value for X compared to the diphenylmethyl radical may be the result of X being more rigid, increasing delocalization, or other structure considerations. Importantly, the fact that **PPA** was not formed in the one-electron region of Figure 4 indicates that the formation of the carbanion is essential to the formation of **PPA**.

In the homogeneous single-electron reduction of **DPA-O$_2$**, the *O*-neophyl-type rearrangement occurs quantitatively because the second ET reduction to $^{\bullet}O-R-R-O^{-}$ to ultimately yield **DPA-(OH)$_2$** is limited by a second diffusional encounter by

(66) Falvey, D. E.; Khambatta, B. S.; Schuster, G. B. *J. Phys. Chem.* **1990**, *94*, 1056−1059.
(67) Amatore, C.; Savéant, J.-M. *Electroanal. Chem.* **1981**, *123*, 221.
(68) Lund, H.; Daasbjerg, K.; Occhialini, D.; Pedersen, S. U. *Acta Chem. Scand.* **1997**, *51*, 135−144.
(69) Wayner, D. D. M.; McPhee, D. J.; Griller, D. *J. Am. Chem. Soc.* **1988**, *110*, 132−137.
(70) Griller, D.; Simões, J. A. M.; Mulder, P.; Sim, B. A.; Wayner, D. D. M. *J. Am. Chem. Soc.* **1989**, *111*, 7872−7876.
(71) Daasbjerg, K.; Pedersen, S. U.; Lund, H. In *General Aspects of the Chemistry of Radicals*; Alfassi, Z. B., Ed.; John Wiley & Sons: Toronto, 1999; pp 385−427.

another donor. We attempted to remove the need for the second diffusional encounter by using the dianion (D^{2-}) donors that undergo a two successive oxidation reaction where the second ET step occurs much more rapidly than the first. The dianions of the donors chosen, 11,11′,12,12′-tetracyanoanthraquinodimethane (**TCAQ**), tetrakis-4-nitrophenylethylene (**TNPE**), and tetrakis-dimethylaminoethylene (**TDAE**), have structural characteristics that allow the second oxidation step to occur at a higher driving force and, hence, faster rate than the first ET. A more thorough explanation of potential inversion and the structural requirements needed for this to occur is given in several accounts by Evans and co-workers.[72−75] The quantitative presence of the rearrangement product when **DPA-O$_2$** is reduced with these two-electron homogeneous donors (and not **DPA-(OH)$_2$**) where the second ET reaction occurs under the conditions of potential inversion provides support for the short vibrational timescale of the rearrangement.

The overall mechanism of homogeneous reduction can also be summarized by Scheme 2, where the e- is a homogeneous donor (e.g., D radical anion or dianion). For the donors in the two-electron reduction region of Figure 4, **PPA** is produced quantitatively through a dissociative ET, followed by rearrangement to X, and then through a second ET that leads to the formation of the dianion product (or semiprotonated equivalent) that eventually forms **PPA** upon workup. For donors with oxidation potentials in the one-electron region, ET leads to the distonic radical anion that rearranges to the carbon-centered radical without further reduction; i.e., X does not get reduced.

The proposed mechanism is also consistent with what is observed in the cyclic voltammetry. On the forward scan in a cyclic voltammogram, the R^1 wave is broad and poorly defined and moves to negative values as the scan rate is increased until completely disappearing at 75 V·s^{-1}. This wave is assigned to the reduction of **PPA** that is being introduced very slowly into the diffusion layer of the electrode. This slow introduction is indicative of a slow rate constant for production of **PPA**, suggesting that there is a slow or rate-determining step in its production. The studies of the **PPA** product wave in the presence of different acids can explain the behavior of the R^2 wave and give information related to the mechanism of formation of **PPA**. Under voltammetric conditions, a small proportion of the **DPA-O$_2$** being reduced rearranges, and the resulting carbon-centered radical is reduced to the carbanion. There are two anionic centers in this intermediate: an alkoxide anion and the carbanion. The data suggests that protonation of these two centers is key to understanding the elimination mechanism and formation of **PPA**.

To investigate this aspect, several acids were chosen so that protonation of either center was favorable by at least five pK_A units. The pK_A values in DMF and ACN for the acids used were estimated from their pK_A in DMSO[76] by applying the relationship pK_A(DMF) = 1.56 + 0.96 pK_A(DMSO)[77] and pK_A(ACN) = 7.10 + 1.17 pK_A(DMSO).[47] The acids used and their corresponding pK_a values in DMF and ACN are phenol (18.4, 28.2), DBP (17.7, 26.8), TFE (24.1, 34.5), acetanilide (22.3, 32.2), water (31.7, 43.8), methanol (31.5, 41.0), and HFIP (20.4, 30.7). There is no known value for pK_B of the alkoxide anion or the structurally similar triphenylmethyl alkoxide anion. Maran and co-workers have estimated the pK_A of the structurally similar triphenylmethyl alcohol to be 31.5 in DMF and 43.5 in ACN based on substituent effects and the acidity scale for alcohols, and this value was used in considering the particular acids used in this study.[48] The carbanion pK_B is also not known. The pK_A of 9,10-dihydroanthracene has been estimated to be 27 in DMSO,[78] and in this case the phenoxy group is expected to increase this value. On the basis of thermodynamic grounds, with the exception of water and methanol, the acids were chosen to safely assume that protonation at both centers of the dianion is expected to be quantitative.

According to the mechanism in Scheme 2, protonation of the alkoxide anion portion is *required* for elimination of hydroxide and formation of **PPA**. Protonation of both centers results in trapping of an intermediate Y, and **PPA** is not formed directly. With the estimated pK_A values, protonation of the carbanion is favored over the alkoxide anion, although this will lead to trapping of the dianion intermediate and stop the formation of **PPA**. However, protonation of the carbanion is expected to be hindered sterically because of the peri interactions of the outer rings of the anthracene backbone, and protonation requires a change in geometry of the reacting carbon center from sp^2 to sp^3 that adds to the kinetic barrier of this proton transfer considerably.[79] Evidence for the slow protonation of the carbanion was verified with the different acids chosen, and the results illustrated in Figure 3 indicate preferential kinetic protonation of the alkoxide anion that leads to the formation of **PPA** via an $E1_{CB}$-type elimination. The small amount of **PPA** that is produced in the absence of any added proton source likely results from water present in the solvents as an impurity. Even in the driest experiments the amount of water is still in the 0.5−1 mmol·L^{-1} range, a comparable concentration to the 2 mmol·L^{-1} **DPA-O$_2$**. Although water is not a thermodynamically favorable acid, it is sufficiently acidic to protonate the alkoxide anion very slowly and allows the irreversible elimination of hydroxide to occur. Thus, from these experiments it is concluded that the elimination of hydroxide is the rate-determining step in the production of **PPA** and is responsible for the totally irreversible electrode behavior observed with the R^1 wave.

Water, methanol, and acetonitrile are the least thermodynamically favorable acids used to protonate the carbon-centered anion. The **PPA** peak height in the voltammetry experiments has the same behavior when DMF and acetonitrile are used as the solvent, suggesting that protonation by acetonitrile is not occurring. The auto protolysis constant of acetonitrile (43.7) is close to the pK_A of water and methanol in acetonitrile, and therefore it is not surprising that at all concentrations of these acids there was also no change in the R^1 peak height, indicating that protonation of the carbanion does not occur from these acids.

Phenol and TFE had no effect on the **PPA** wave until two or more equivalents were added, which caused the peak to disappear. It is conceivable that the small size of TFE and phenol

(72) Evans, D. H. *Chem. Rev.* **1990**, *90*, 739−751.
(73) Evans, D. H. *Acta Chem. Scand.* **1998**, *52*, 194−197.
(74) Evans, D. H.; Hu, K. *J. Chem. Soc., Faraday Trans.* **1996**, *92*, 3983−3990.
(75) Evans, D. H.; Lehmann, M. W. *Acta Chem. Scand.* **1999**, *53*, 765−774.
(76) Bordwell, F. *Acc. Chem. Res.* **1988**, *21*, 456−463.
(77) Maran, F.; Celadon, D.; Severin, M. G.; Vianello, E. *J. Am. Chem. Soc.* **1991**, *113*, 9320−9329.
(78) Parker, V. D.; Tilset, M.; Hammerich, O. *J. Am. Chem. Soc.* **1987**, *109*, 7905−7906.
(79) Andrieux, C. P.; Savéant, J.-M.; Tardy, C. *J. Electroanal. Chem.* **1999**, *476*, 81−84.

Scheme 3. Proposed Mechanism of Fe(II) Reduction of **DPA-O_2**

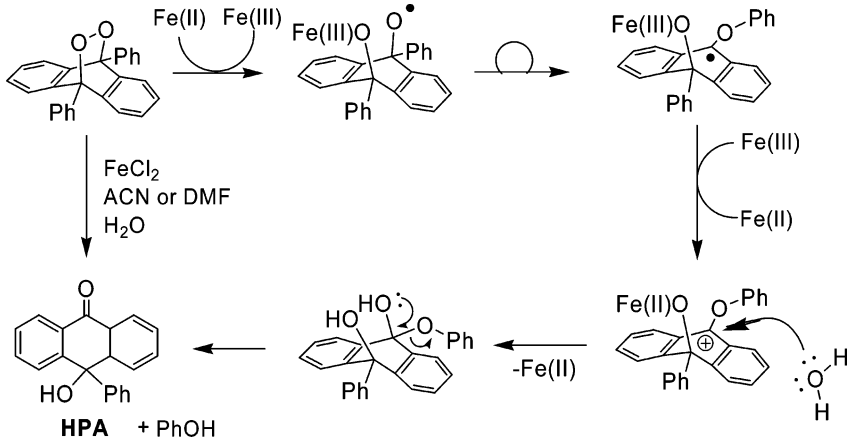

allow them to protonate the alkoxide anion easily and, in the presence of 2 equiv, protonate the carbanion as well, shutting off the elimination mechanism by trapping the dianion intermediate Y. In contrast, the larger structural analogues of these acids, DBP and HFIP, did not quench formation of **PPA** completely. This we attribute to these larger acids being sufficient to protonate the carbanion on thermodynamic grounds but unable to do so kinetically. Acetanilide and TFE have nearly identical pK_A values, and the only other difference between these two is their structure and corresponding steric bulk. Yet with acetanilide, there is no loss of the **PPA** wave at any of the concentrations investigated, suggesting that protonation of the carbanion does not occur. The voltammetry in the presence of these acids is consistent with kinetic protonation of the alkoxide anion occurring over the more thermodynamically favorable protonation of the carbanion. This allows for the irreversible rate-determining elimination reaction of hydroxide to occur and to form **PPA** before the second protonation of the carbanion.

The characteristics of the cyclic voltammetry of **DPA-O_2** illustrated in Figure 2 can now be explained in terms of the proposed mechanism. In Figure 2a, as the potential is scanned through the dissociative wave, a small proportion of the distonic radical anion produced undergoes the *O*-neophyl-type rearrangement to produce the carbon-centered radical X. This radical is reduced to the carbanion that undergoes elimination of hydroxide on protonation of the alkoxide anion to form **PPA**. As the potential is scanned to more negative values, the small amount of **PPA** made at the electrode surface is converted to the **PPA** radical anion, **PPA**$^{\bullet-}$, that catalytically reduces the **DPA-O_2** that is moving toward the electrode surface. The yield of **PPA** observed in the voltammogram is dependent on the rate of formation of **PPA** and the amount of time spent at potentials where it is reduced to its radical anion. This explains why the peak O^2 is larger than R^1 and why the yield of **PPA** in cyclic voltammetry of **DPA-O_2** is greater than the 3% yield observed under preparative reduction conditions between -1.1 and -1.5 V vs SCE. Under the conditions of the experiment in Figure 2d, it is possible to obtain an essentially quantitative yield of **PPA**, based on the peak height, by the homogeneous redox catalysis by **PPA**$^{\bullet-}$ which is an efficient catalytic ET donor reducing the incoming **DPA-O_2** and effectively shut down the heterogeneous reduction. Under purely homogeneous ET conditions, the *O*-neophyl-type rearrangement pathway and formation of **PPA** occurs quantitatively at <-0.9 V vs SCE. In the presence of a suitable acid, the carbanion formed is trapped and stops the $E1_{CB}$ type elimination of hydroxide to form **PPA**.

Scheme 4. Proposed Mechanism of Fe(II) Reduction of **DMA-O_2**

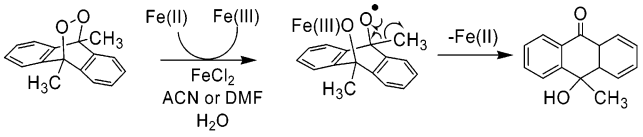

Iron(II)-induced fragmentation of the O−O bond of cyclic peroxides has been well-studied.[32,80,81] In the case of **DPA-O_2**, the results of Fe(II)-induced cleavage is consistent with the *O*-neophyl-type rearrangement occurring quantitatively under these homogeneous conditions. A proposed mechanism for the reduction of **DPA-O_2** by ferrous ion accounting for the observed product is shown in Scheme 3. The *O*-neophyl-type rearrangement of the initially formed alkoxy radical leads to the carbon-centered radical. Back ET from the carbon radical to the Fe(III) can occur to generate a carbocation and Fe(II); this is similar to that observed in other systems and explains why only a catalytic amount of the $FeCl_2$ is required. The carbocation then can undergo a nucleophilic attack by water followed by elimination of phenoxide (phenol) to give **HPA**. The Fe(II)-mediated reduction of **DMA-O_2** leads to the alkoxy radical that undergoes a β-scission reaction to extrude a methyl radical and form the anthrone in a single step as shown in Scheme 4. The rearrangement rate constant for the 1,2-methyl shift that would be analogous to the *O*-neophyl rearrangement is not known and is assumed not to be competitive with the β-scission reaction that has a minimum rate constant of 4.4×10^6 s^{-1}.[82−85] In contrast, these β-scission reactions do not occur in the heterogeneous reduction because the second ET to the alkoxy radical is very rapid since it is generated at the electrode.

Conclusion

The initial ET reduction **DPA-O_2** and **DMA-O_2** follows a dissociative mechanism with fragmentation of the O−O bond

(80) Szpilman, A. M.; Korshin, E. E.; Hoos, R.; Posner, G. H.; Bachi, M. D. *J. Org. Chem.* **2001**, *66*, 6531−6540.
(81) Wu, W.-M.; Wu, Y.; Yao, Z.-J.; Zhou, C.-M.; Li, Y.; Shan, F. *J. Am. Chem. Soc.* **1998**, *120*, 3316−3325.
(82) Griller, D.; Ingold, K. U. *Acc. Chem. Res.* **1980**, *13*, 193−200.
(83) Griller, D.; Ingold, K. U. *Acc. Chem. Res.* **1980**, *13*, 317−323.
(84) Arends, I. W. C. E.; Ingold, K. U.; Wayner, D. D. M. *J. Am. Chem. Soc.* **1995**, *117*, 4710−4711.
(85) Avila, D. V.; Brown, C. E.; Ingold, K. U.; Lusztyk, J. *J. Am. Chem. Soc.* **1993**, *115*, 466−470.

to yield a distonic radical anion. Under the conditions of ET and thus at the transition state whereby the O−O bond is stretched with respect to the equilibrium length, the LUMO of these molecules has a strong contribution of the σ*-orbital associated with the O−O bond. The subsequent reactivity of the distonic radical anion formed on reduction of **DPA-O$_2$** can be controlled by using either homogeneous or heterogeneous methods. Under homogeneous conditions, the initial dissociative ET is followed by a rapid *O*-neophyl-type rearrangement that leads to the formation of *O*-insertion products for **DPA-O$_2$**. Under heterogeneous reduction conditions, the *O*-neophyl-type rearrangement competes with the highly driven second ET reduction of the distonic radical anion formed at the electrode surface that yields the corresponding 9,10-diol after protonation. In either case, after rearrangement, the formation of the carbon-centered radical leads to the formation of **PPA** through a cascade of steps that involves its reduction followed by selective protonation of the alkoxide anion portion of the singly reduced intermediate. The reduction of this radical depends on the potential of the reducing media and allows for the estimation of its reduction potential (−0.85 V vs SCE). A unified mechanism that accounts for the differences observed in the homogeneous and heterogeneous ET chemistry has been proposed.

Under the ET conditions, reduction of **DPA-O$_2$** follows different reaction pathways compared to either thermal or photochemical activation. For example, there is no evidence for C−O activation upon ET that is observed in the photochemical and thermolysis studies of these compounds. By constructing activation driving force relationships for the heterogeneous ET process and applying it to the current theories of dissociative ET, the intrinsic barrier for the bond-breaking ET process was determined along with several other important and previously undetermined thermochemical parameters. An interesting aspect of this is that there appears to be significantly lower solvating energy required for the reduction of **DPA-O$_2$** compared to **DMA-O$_2$** that we attributed to added shielding by the adjacent phenyl rings. Another outcome of the analysis is estimates for the BDE of the O−O bond in **DPA-O$_2$** (and **DMA-O$_2$**); they represent some of the lowest of any O−O BDE yet reported.[86] Therefore, a question that can arise is why does the C−O bond fragment in preference to the weaker O−O bond under some conditions? A possible explanation is that there is an extra kinetic barrier to the fragmentation of the O−O bond related to an inherent nonadiabaticity due to a failure of the Born−Oppenheimer approximation near the transition state for O−O cleavage.[87] It is now established that ET to O−O bonded systems is nonadiabatic,[49,52,63,88,89] and evidence for this in **DPA-O$_2$** and **DMA-O$_2$** systems is noted by the low magnitude of the k_{het}^{o} values.

Acknowledgment. This work was supported financially by the Natural Sciences and Engineering Research Council of Canada, Canadian Foundation for Innovation, the Ontario Research and Development Challenge Fund, a Premier's Research Excellence Award, and an ADF New Research and Scholarly Initiatives Award of the University of Western Ontario. R.L.D. is grateful for an NSERC post graduate scholarship. Dr. M. C. Jennings performed the X-ray crystallographic analysis, and Doug Hairsine performed the mass spectroscopic analyses. Professor Flavio Maran is thanked for his valuable scientific insights.

Supporting Information Available: The Experimental Section, including experimental details and spectral characterization of all compounds and product studies, tables of crystallographic data, and details of the convolution analysis (PDF, CIF). This material is available free of charge via the Internet at http://pubs.acs.org.

JA035828A

(86) Luo, Y.-R. *Handbook of Bond Dissociation Energies in Organic Compounds*; CRC Press: Boca Raton, FL, 2003.
(87) Butler, L. J. *Annu. Rev. Phys. Chem.* **1998**, *49*, 125−171.
(88) Antonello, S.; Formaggio, F.; Moretto, A.; Toniolo, C.; Maran, F. *J. Am. Chem. Soc.* **2001**, *123*, 9577−9584.
(89) Antonello, S.; Crisma, M.; Formaggio, F.; Moretto, A.; Taddei, F.; Toniolo, C.; Maran, F. *J. Am. Chem. Soc.* **2002**, *124*, 11503−11513.